

*Supporting Information*

# **Separating Convective from Diffusive Mass Transport Mechanisms in Ionic Liquids by Redox Pro-fluorescence Microscopy**

Mattia Belotti,<sup>a</sup> Mohsen M. T. El-Tahawy,<sup>b,c</sup> Marco Garavelli,<sup>b</sup> Michelle L. Coote,<sup>d</sup> K.  
Swaminathan Iyer,<sup>e</sup> and Simone Ciampi<sup>\*,a</sup>

<sup>a</sup> School of Molecular and Life Sciences, Curtin University, Bentley, Western Australia 6102, Australia; Email:  
simone.ciampi@curtin.edu.au

<sup>b</sup> Dipartimento di Chimica Industriale “Toso Montanari”, Università di Bologna, Bologna, Emilia Romagna, 40136, Italy

<sup>c</sup> Chemistry Department, Faculty of Science, Damanhour University, Damanhour 22511, Egypt

<sup>d</sup> Institute for Nanoscale Science and Technology, College of Science and Engineering, Flinders University Bedford Park,  
South Australia, 5042, Australia

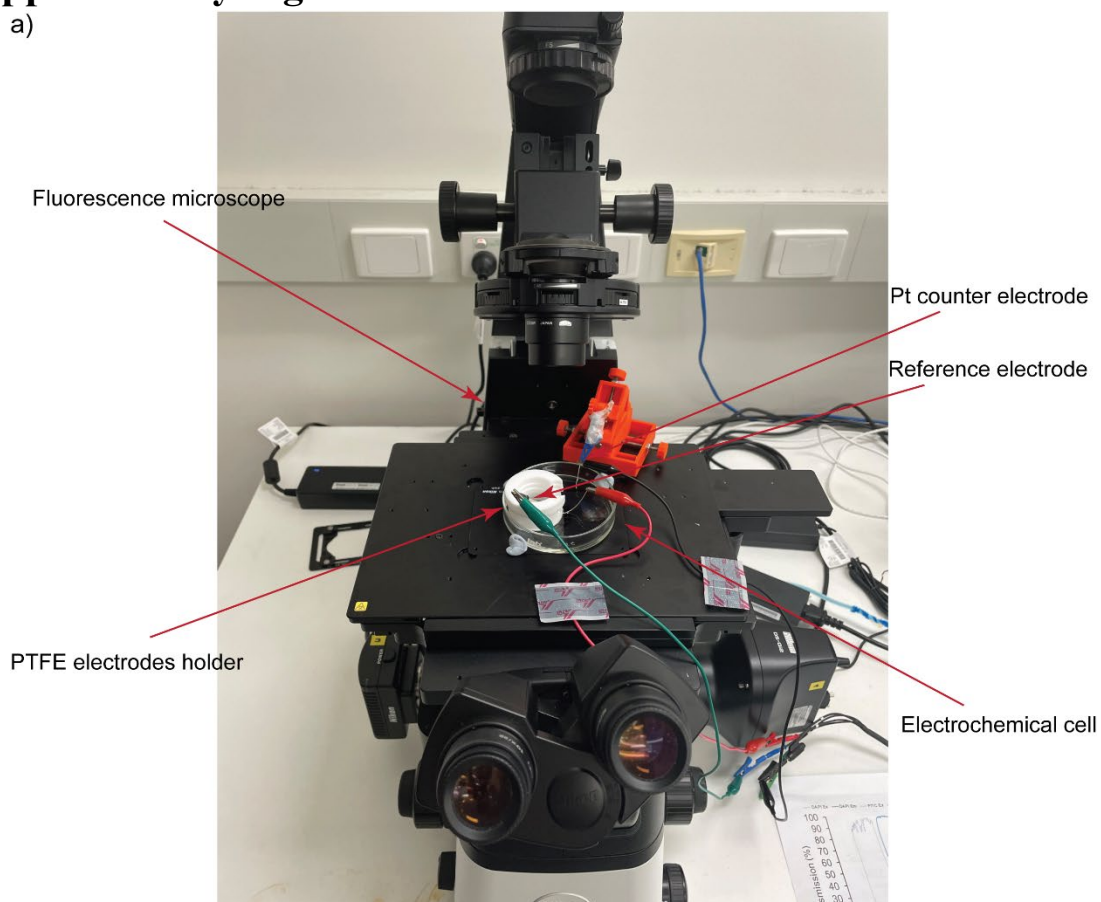
<sup>e</sup> School of Molecular Sciences, The University of Western Australia, Perth, Western Australia 6009, Australia

## **Table of Contents**

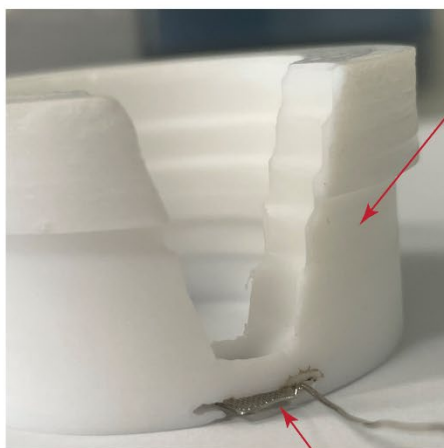
<b>Supplementary Figures .....</b>	<b>2</b>
<b>Description of Supplementary Videos.....</b>	<b>23</b>
<b>References .....</b>	<b>25</b>

## Supplementary Figures

a)



b)



c)



**Figure S1.** Experimental setup for the collection of ECL and fluorescence time-resolved micrographs. (a) A Petri dish, resting on the sample stage of an inverted fluorescence microscope, is loaded with the electrolytic solution and fitted with a custom PTFE electrodes holder. (b) Side view of the PTFE electrode holder showing the horizontal slot for the Pt mesh working electrode. The platinum mesh position is sitting parallel and ~2 mm away from the bottom glass surface of the Petri dish. (c) Bottom view of the PTFE holder.

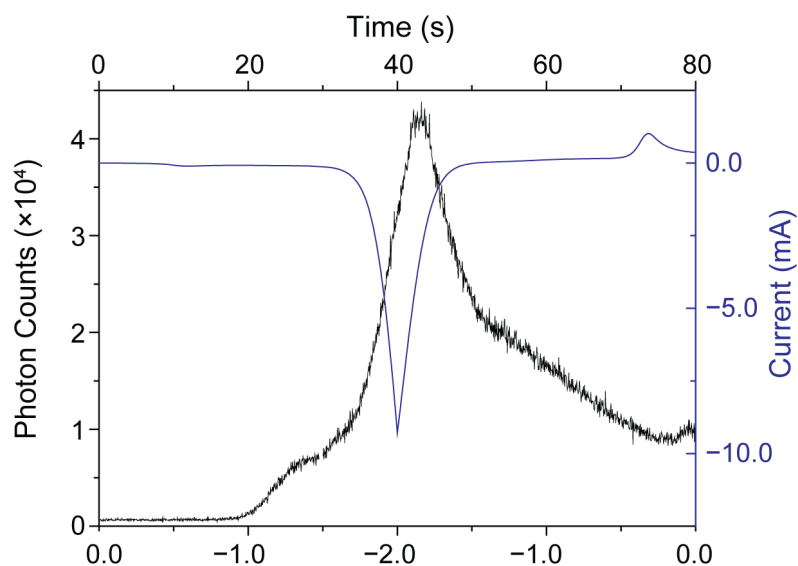


**Figure S2.** Overlaid plots of simultaneously acquired photon counts (black trace) and current (blue trace) during the cathodic electrolysis at a platinum mesh electrode of an  $0.4 \times 10^{-3}$  M **AMP-luc** oxygen-saturated solution in [EMIM][EtSO<sub>4</sub>]. The potential was swept cyclically from 0.0 V to -2.0 V, and back, at a scan rate of 0.05 V/s. The emission peak corresponds to  $\sim 4.20 \times 10^4$  photon/s.

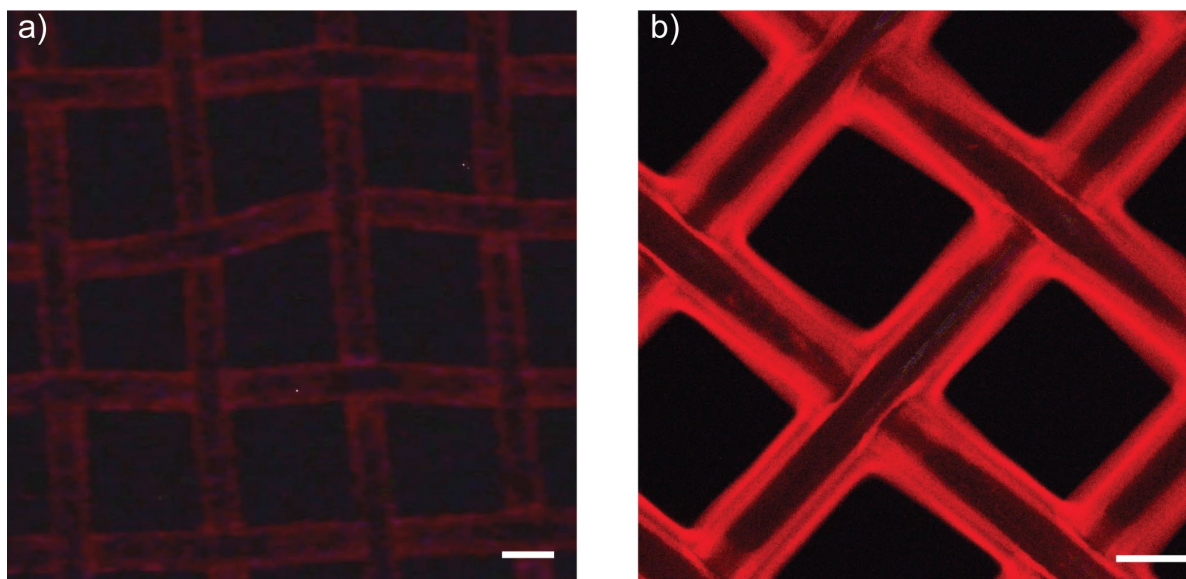


**Figure S3.** Full field of view for the ECL micrographs shown partially cropped in Figure 1b of the main text. (a) The ECL image was captured in a dark room,  $\sim 2.0$  s after a  $-2.0$  V cathodic pulse (30 s long) is applied to a Pt mesh immersed in a  $0.4 \times 10^{-3}$  M **AMP-luc** oxygen-saturated solution in [EMIM][EtSO<sub>4</sub>]. (b) A similar experiment as in (a) but carried out in a molecular solvent-based electrolyte ( $0.4 \times 10^{-3}$  M **AMP-luc** in oxygen-saturated 0.2 Bu<sub>4</sub>NClO<sub>4</sub>/DMSO, Video S1). The micrograph shown in (a) is edited to maximise contrast. Scale bars are 100  $\mu$ m.

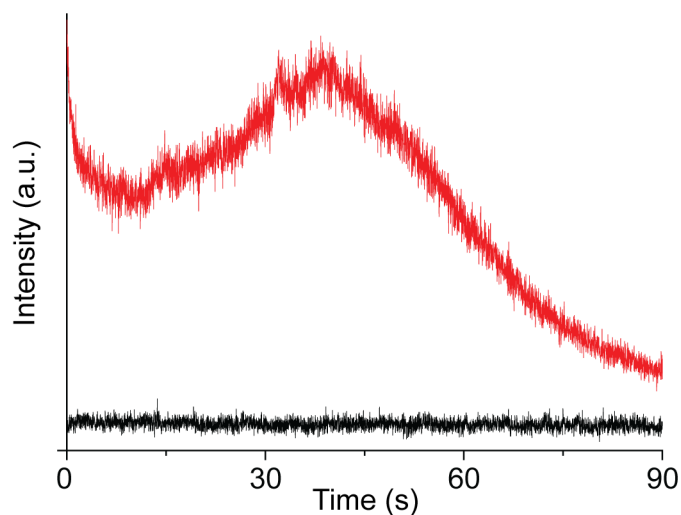


**Figure S4.** Time evolution of the electrochemically generated light emission (ECL) upon the electrolysis at a platinum mesh electrode of an **AMP-luc** solution ( $0.4 \times 10^{-3}$  M in [EMIM][EtSO<sub>4</sub>]). The room temperature ionic liquid solution was either oxygen-saturated (red trace) or argon-saturated (black trace). Electrolytic solutions were bubbled with either oxygen (red trace) or argon (black trace) for at least 20 min prior to the ECL experiments. To trigger the ECL the voltage of the working electrode was stepped from open circuit to  $-2.5$  V vs Ag/AgCl for 30 s. The ECL is monitored at 626 nm (emission slit set to 20 nm). The experiment with the argon-saturated **AMP-luc** solution was performed under positive argon pressure and with a small amount of oxygen scavenger (ammonium sulfite 0.5 % w/v) added to the solution.

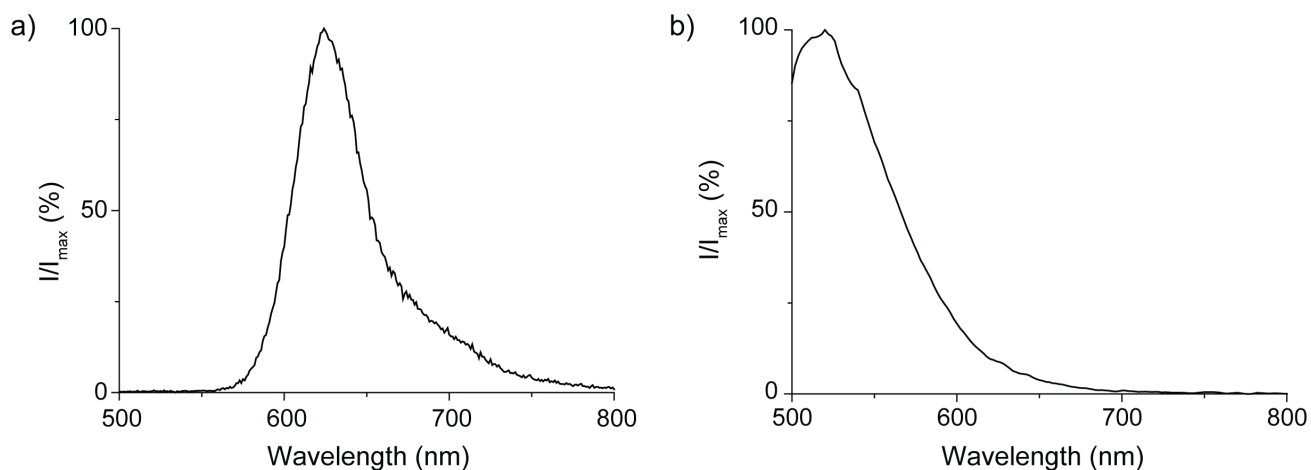


**Figure S5.** (a) Spectrum of the chemically induced **AMP-luc** luminescence. Argon gas was bubbled through an **AMP-luc** solution ( $0.4 \times 10^{-3}$  M, 0.2 M  $\text{Bu}_4\text{NClO}_4/\text{DMSO}$ ) for at least 20 min prior to the experiment. A quartz cuvette ( $10 \times 10 \times 40$  mm) was loaded with  $\text{KO}_2$  (0.02 g) and placed inside the spectrometer sample compartment (Varian, Palo Alto, California). Using silicone tubing (diameter 3.0 mm) **AMP-luc** solution (4 mL) was transferred in one portion from a syringe to the cuvette containing the  $\text{KO}_2$  powder, avoiding ambient light to interfere with the ECL recording. Spectral acquisition started once the injection was completed, and recording a full spectrum took  $\sim 1.5$  s. Throughout all the procedure a gentle flow of argon gas was maintained inside the sample compartment. (b) Fluorescence spectrum recorded  $\sim 30$  s after the **AMP-luc** sample injection to the cuvette containing  $\text{KO}_2$ . The excitation wavelength was set to 474 nm and the emission slit to 20 nm.

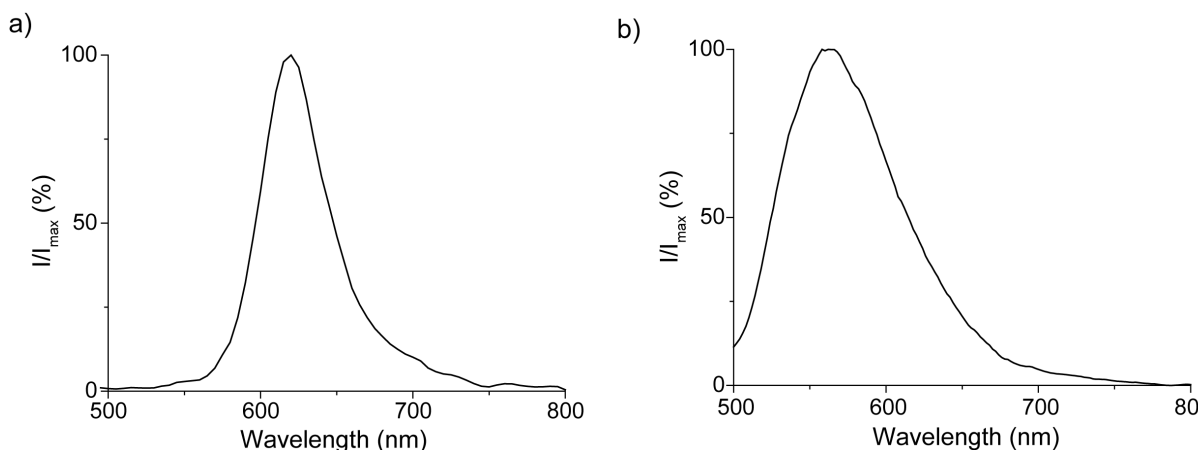


**Figure S6.** (a) Spectrum of the chemically induced **AMP-luc** luminescence. Argon gas was bubbled through an **AMP-luc** solution ( $0.4 \times 10^{-3}$  M in [EMIM][EtSO<sub>4</sub>]) for at least 20 min prior to the experiment. A quartz cuvette (10×10×40 mm) was loaded with KO<sub>2</sub> (0.02 g) and placed inside the spectrometer sample compartment (Varian, Palo Alto, California). Using silicone tubing (diameter 3.0 mm) **AMP-luc** solution (4 mL) was transferred in one portion from a syringe to the cuvette containing the KO<sub>2</sub> powder, avoiding ambient light to interfere with the ECL recording. Spectral acquisition started once the injection was completed, and recording a full spectrum took ~1.5 s. Throughout all the procedure a gentle flow of argon gas was maintained inside the sample compartment. (b) Fluorescence spectrum recorded ~30 s after the **AMP-luc** sample injection to the cuvette containing KO<sub>2</sub>. The excitation wavelength was set to 474 nm and the emission slit to 20 nm.

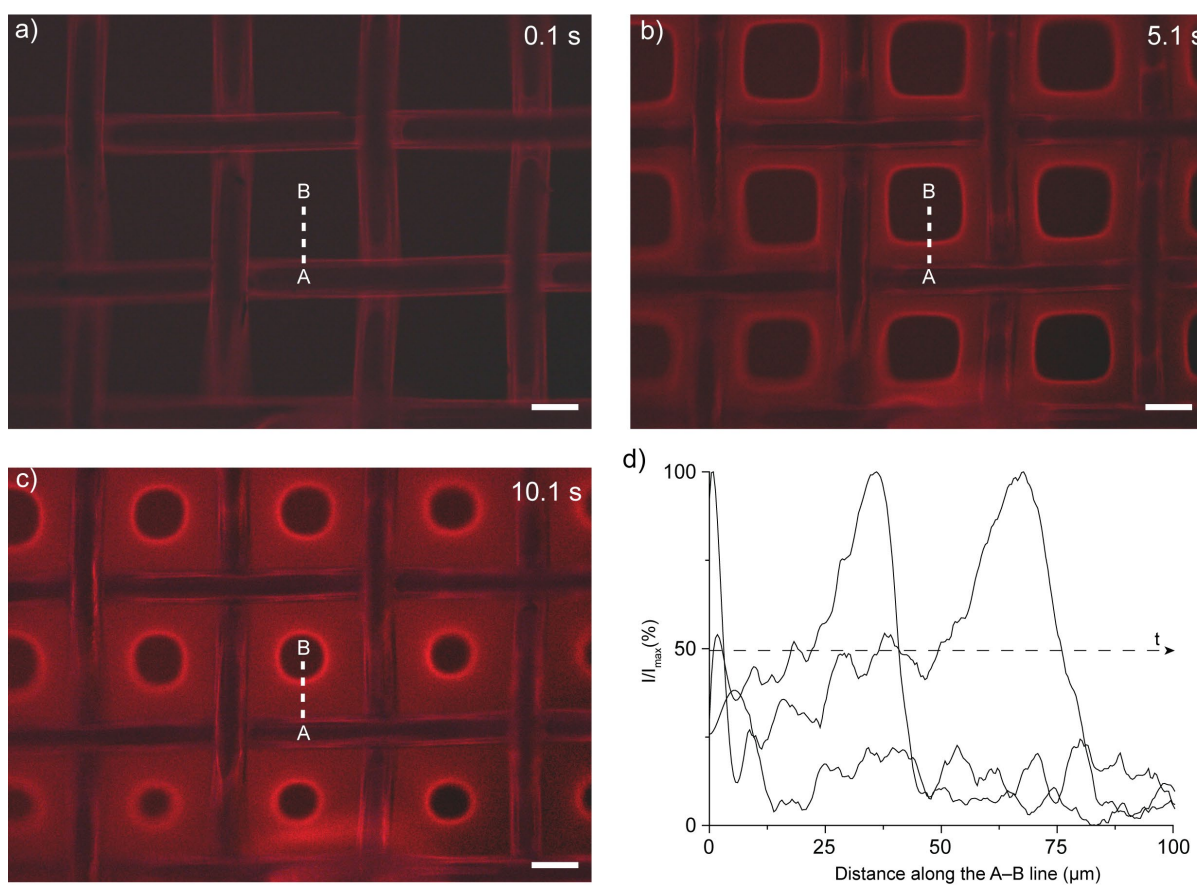


**Figure S7.** (a–c) Selected time-stamped micrographs ( $10\times$  magnification, micrographs edited to maximise contrast, see Video S4) showing the movement of the **AMP-luc** electrochemiluminescent front (diffusion of superoxide away from the Pt mesh electrode where it forms). The electrochemiluminescent reaction is triggered upon the cathodic electrolysis ( $-2.0$  V) of an oxygen-saturated **AMP-luc** solution ( $0.4 \times 10^{-3}$  M) in  $2.0 \times 10^{-1}$  M  $\text{Bu}_4\text{NClO}_4/\text{DMSO}$ . The video was recorded in a dark room and the time stamps (0.1 s (a), 5.1 s (b) and 10.1 s (c)) refer to the time that has elapsed after the working electrode potential is stepped from open circuit to  $-2.0$  V (vs. reference). Scale bars in (a–c) are  $100 \mu\text{m}$ . (d) Electrochemiluminescence profile sampled along the A–B line marked in (a–c), capturing the position of the diffusion front, from electrode’s surface, ( $t$ ) of 0.1, 5.1, and 10.1 s. The optically determined superoxide diffusion coefficient is  $2.62 \times 10^{-6} \text{ cm}^2\text{s}^{-1}$ . Point A is placed approximately on the platinum wire edge (top view).



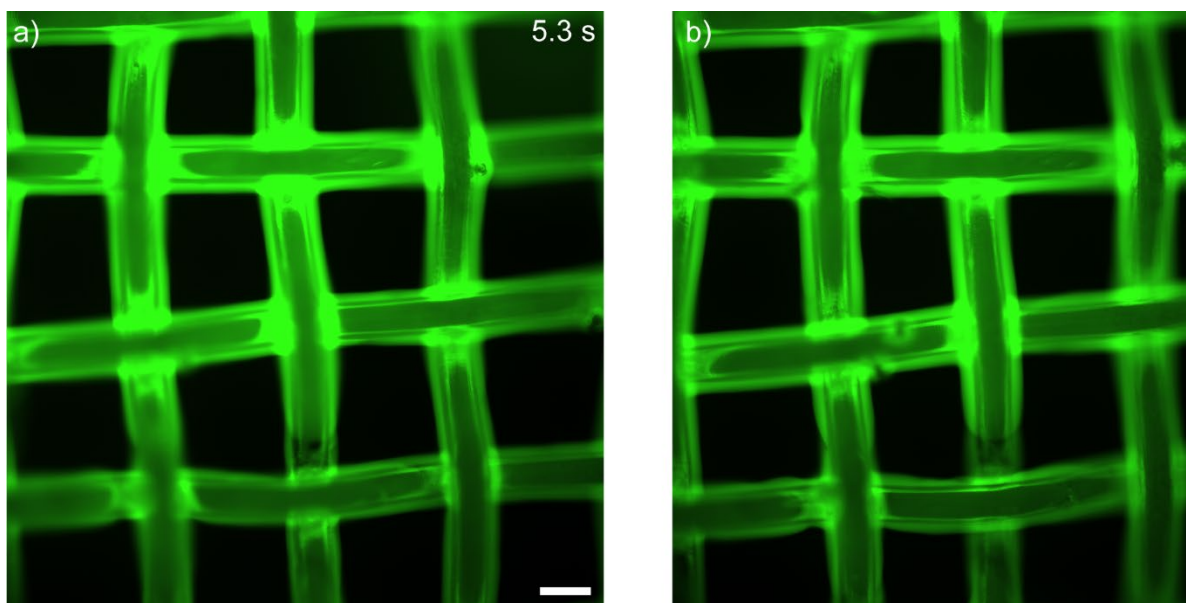


**Figure S8.** Fluorescence micrographs (10× magnification) recorded during the cathodic electrolysis ( $-2.0$  V vs Ag/AgCl) of an oxygen-saturated **AMP-luc** solution ( $0.4 \times 10^{-3}$  M in [EMIM][EtSO<sub>4</sub>]) at a platinum mesh working electrode. The counter electrode (Pt coil) was placed either on the left (a) or on the right side (b) of the working electrode.

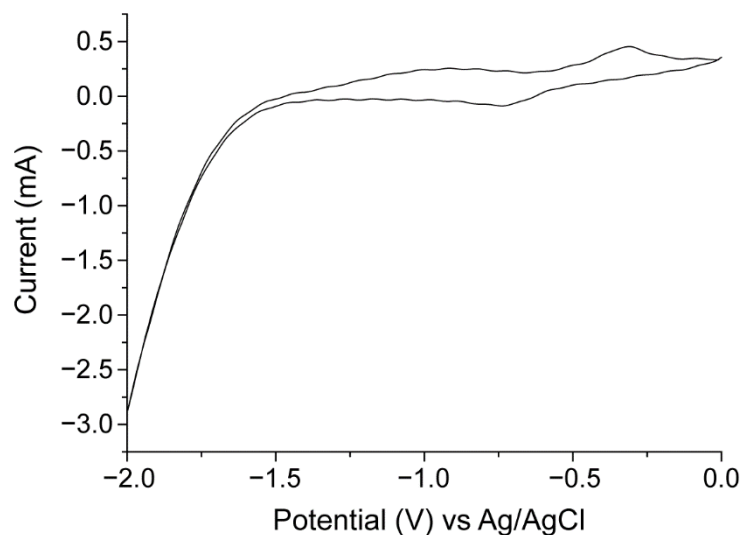


**Figure S9.** Representative cyclic voltammogram (CV) recorded at a platinum mesh electrode in oxygen-saturated [EMIM][EtSO<sub>4</sub>], without **AMP-luc**. The voltage scan rate is 0.05 V/s. In the dynamic CV measurement the oxygen reduction peak is appearing at about -0.7 V vs Ag/AgCl (-1.15 vs Fc/Fc<sup>+</sup>), a potential where overscreening should already be occurring (Figure 2f, main text, onset of overscreening is at approximately -0.75 V vs Fc/Fc<sup>+</sup>). These data suggest that the cation rich-structure effectively slows down inner-sphere reactions (such as hydrogen evolution) only at large negative potentials, where crowding sets in.

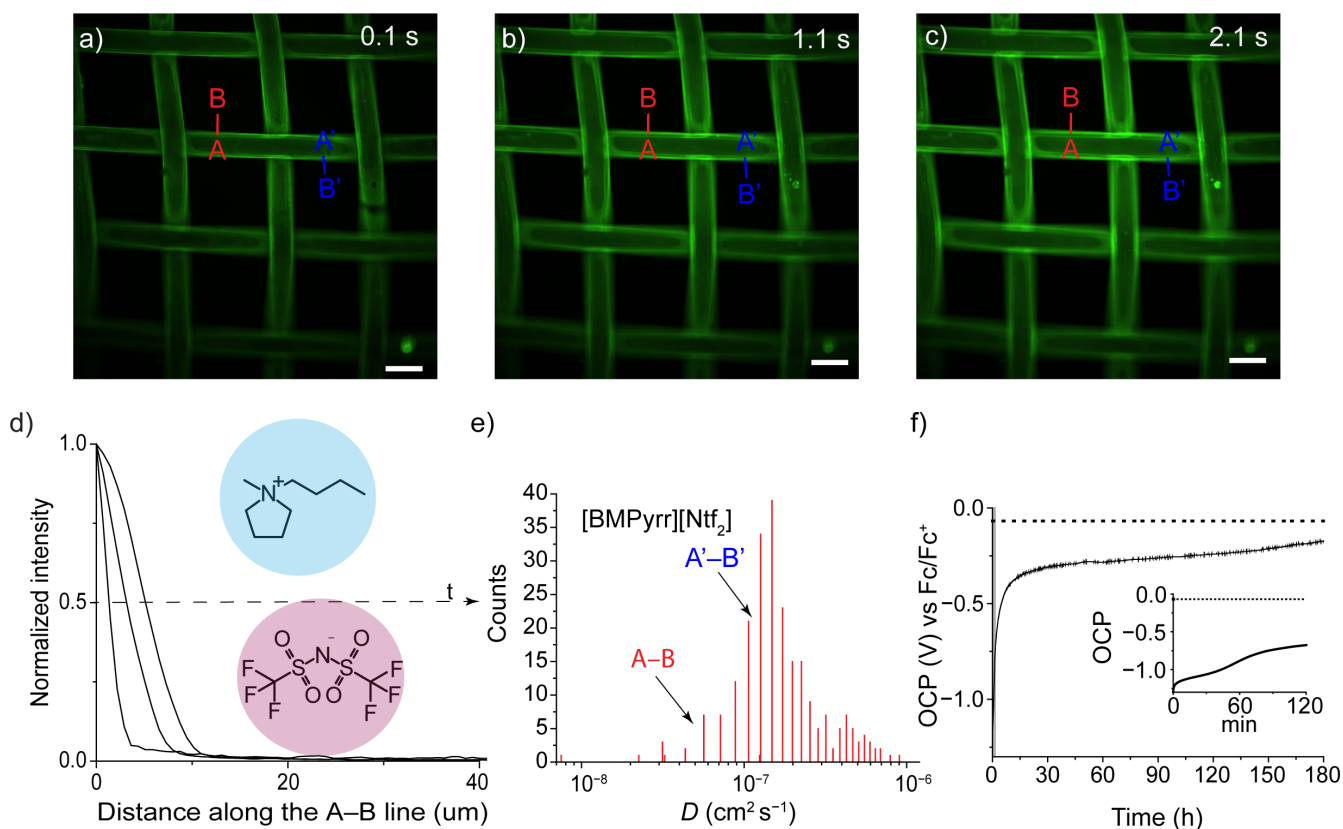


**Figure S10.** (a–c) Selected time-stamped fluorescence micrographs (10× magnification, 461.0–487.5 nm excitation, 502.5–547.5 nm emission, Video S5) capturing the movement of the electrochemically generated *ox-luc*. *ox-luc* is the product of the cathodic electrolysis of an oxygen-saturated **AMP-luc** solution ( $0.4 \times 10^{-3}$  M in [BMPyrr][Ntf<sub>2</sub>]) at a platinum mesh electrode. The time stamps shown in panels (a–c) refer to the time that has elapsed after the working electrode potential is stepped from open circuit to  $-2.0$  V (0.1 s (a), 1.1 s (b) and 2.1 s (d)). Representative fluorescence profiles, sampled along the A–B line, at electrolysis times of 0.1, 1.1 and 2.1 s. The procedure (tracking the movement of the diffusion front) was repeated in at least 20 different locations per experiment, and at least 10 independent experiments were performed. Approximately 200 values of diffusivity were calculated for each system, and the distribution of these values is shown by the histogram in (e). For example, by tracking superoxide diffusion along the A–B line, we obtained a diffusion coefficient (*D*) for superoxide of  $0.40 \times 10^{-7}$  cm<sup>2</sup> s<sup>-1</sup>, while the same approach along the A'–B' line led to a *D* of  $1.10 \times 10^{-7}$  cm<sup>2</sup> s<sup>-1</sup>. Scale bars in (a–c) are 100 μm. The mode of the optically determined superoxide *D* is  $1.30 \times 10^{-7}$  cm<sup>2</sup> s<sup>-1</sup>. (f) Representative OCP–time measurement for a platinum mesh electrode immersed in [BMPyrr][NTf<sub>2</sub>] (125 ppm water content). The OCP logging started after the end of a 60 s negative bias pulse ( $-2.0$  V vs the initial OCP). The dotted line represents the initial OCP. The gray shaded area in (f) indicates the data plotted in the figure inset. This inset reveals the onset of crowding between  $-1.0$  V and  $-1.2$  V. The overscreening OCP signature (plateau in OCP) lays between  $-0.25$  V and  $-0.35$  V.

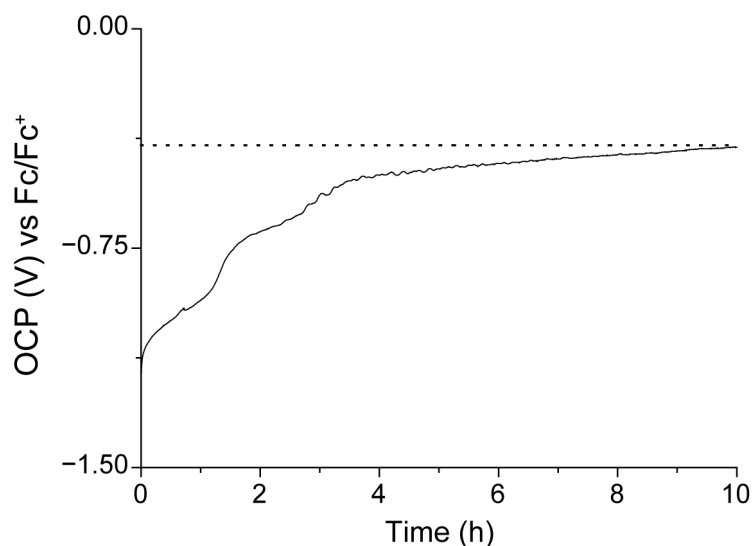


**Figure S11.** Representative OCP–time measurement of a platinum mesh electrode immersed in [EMIM][BF<sub>4</sub>]. The OCP measurement was started after the end of a 60 s cathodic pulse (–2.0 V away from the system’s initial OCP). The dotted horizontal line represents the initial OCP before the cathodic pulse.

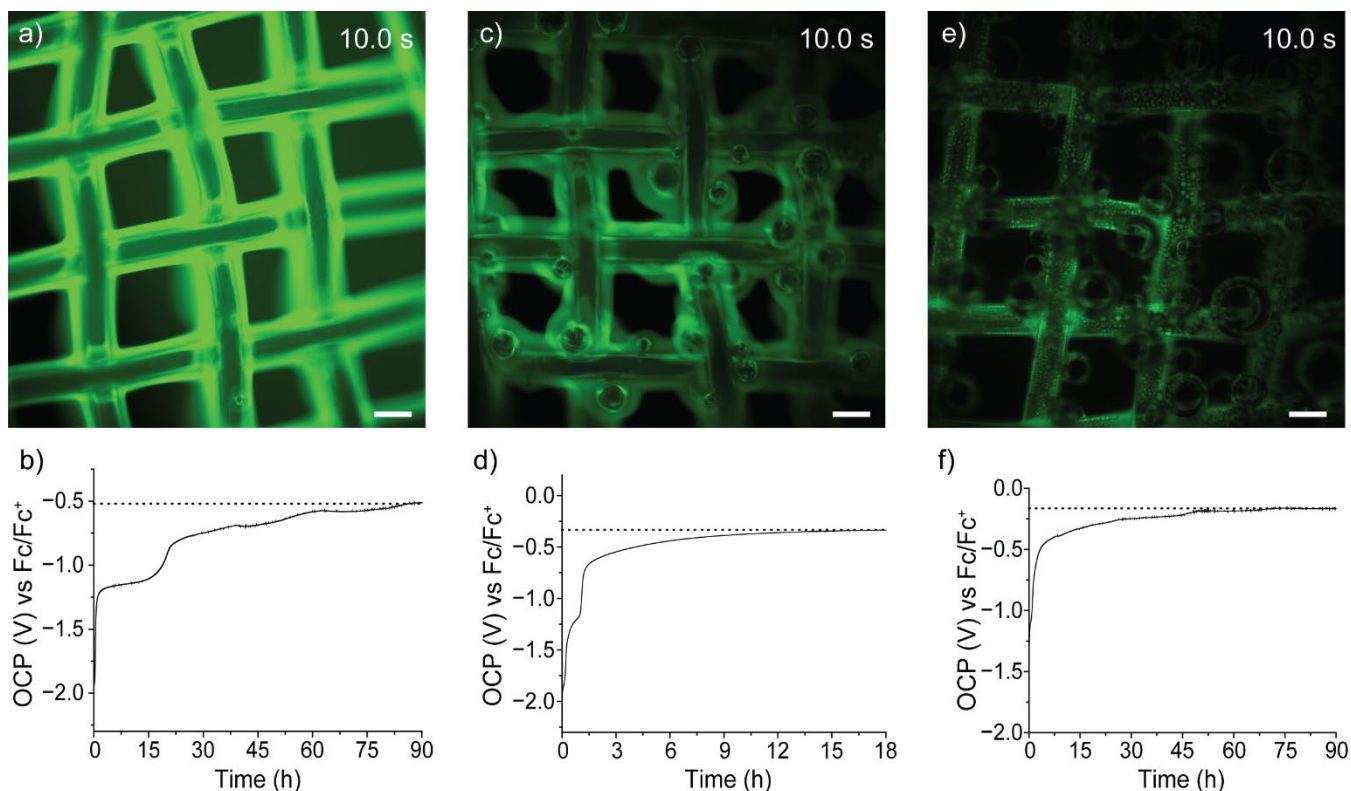


**Figure S12.** (a,c,e) Selected time-stamped fluorescence micrographs recorded 10 s after the working electrode potential is stepped cathodically ( $-2.0$  V) away from open circuit ( $10\times$  magnification  $461.0\text{--}487.5$  nm excitation,  $502.5\text{--}547.5$  nm emission). The fluorescence images capture the evolution of gases upon the electrolysis of oxygen-saturated **AMP-luc** solutions ( $0.4 \times 10^{-3}$  M) in various RTILs. The RTIL in (a) and in (c) is [EMIM][EtSO<sub>4</sub>], spiked respectively with either 2.0% (a) or 5% (c) of water (Videos S6–S7). The RTIL in (e) is [BMPyrr][NTf<sub>2</sub>], spiked with 2.0% of water (Video S8). (b,d,f) OCP–time measurement for the mesh platinum electrode immersed in the RTIL systems of (a), (c) and (e). The OCP was recorded after the application of  $-2.0$  V relative to the system’s initial OCP.

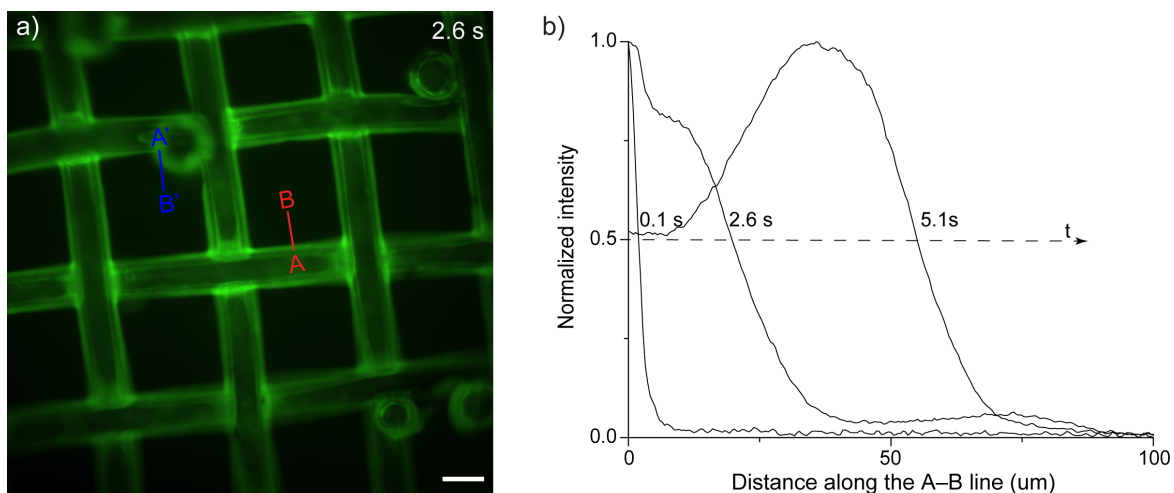


**Figure S13.** Selected time-stamped fluorescence micrograph (10 $\times$  magnification) recorded during the cathodic electrolysis ( $-2.0$  V vs Ag/AgCl) of an oxygen-saturated **AMP-luc** solution ( $0.4 \times 10^{-3}$  M in [EMIM][BF<sub>4</sub>]). (b) Representative fluorescence intensity plot profiles sampled along the A'–B' line marked in (a) and in Figure 3a–b, recorded 0.1, 2.6 and 5.1 s after the working electrode bias is stepped from open circuit to  $-2.0$  V, used for the analysis of the movement over time of the superoxide diffusion front (triggering the **ox-luc** formation). The  $D$  values reported in the main text are calculated from the front distance travelled after 5.1 s, and are therefore an average apparent diffusivity during this time, but as data in (b) show, the apparent diffusion is not uniform over time, with the front progressing faster as the bubbles become larger.

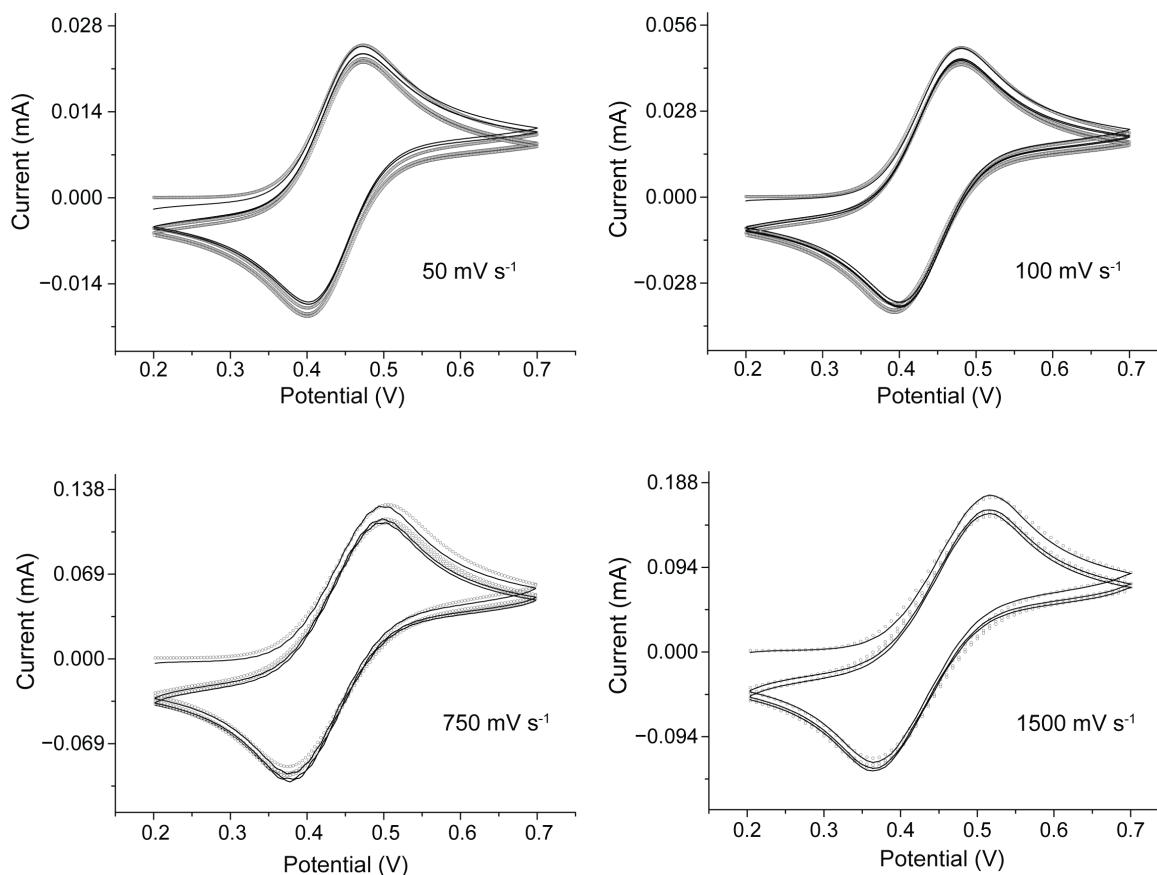


**Figure S14.** Representative experimental (solid line) and simulated (empty symbols) cyclic voltammograms recorded at a platinum disk electrode in an acetonitrile solution containing  $1.0 \times 10^{-3}$  M ferrocene and  $1.0 \times 10^{-1}$  Bu<sub>4</sub>NPF<sub>6</sub>. The voltage sweep rate is indicated as a label to the figures. The diffusivity ( $D$ ) of ferrocene and ferricenium (Fc and Fc<sup>+</sup> hereafter) was set to  $2.60 \times 10^{-5}$  cm<sup>2</sup> s<sup>-1</sup>. The best-fit parameters (E mechanism) are  $E^0$  (Fc/Fc<sup>+</sup>) = 0.4371 V (vs. Ag/AgCl “leakless”, upper limit 0.4374, lower limit 0.4368, 95.4% confidence level), and  $k_{\text{et}} = 0.040$  cm s<sup>-1</sup> (upper limit 0.043, lower limit 0.037, 95.4% confidence level). The electrochemically-determined effective area of the platinum disk is 0.08 cm<sup>2</sup>.

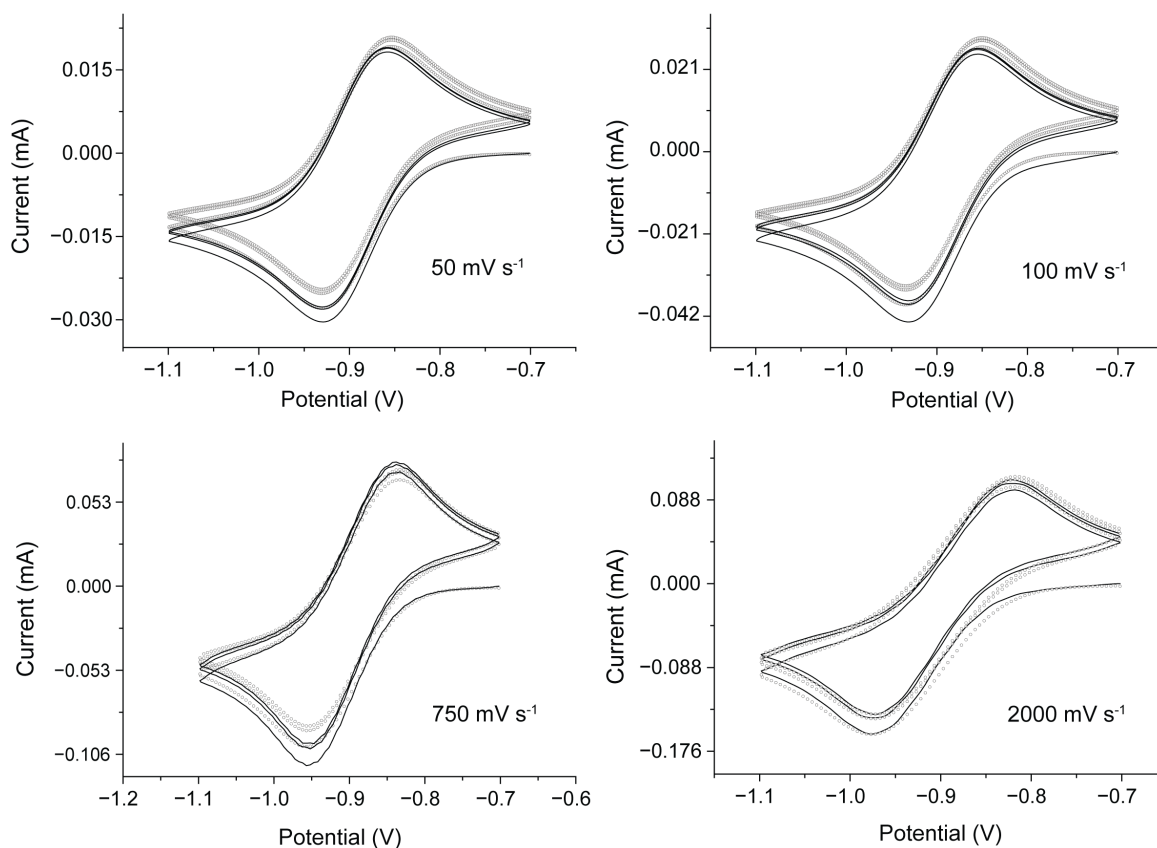


**Figure S15.** Representative experimental (solid line) and simulated (empty symbols) cyclic voltammograms recorded at a platinum disk electrode in an acetonitrile solution containing  $1.0 \times 10^{-3}$  M cobaltocenium hexafluorophosphate and  $1.0 \times 10^{-1}$  Bu<sub>4</sub>NPF<sub>6</sub>. The voltage sweep rate is indicated by labels to the figures. The  $D$  of cobaltocene and cobaltocenium (Cc and Cc<sup>+</sup> hereafter) was set to  $3.25 \times 10^{-5}$  cm<sup>2</sup> s<sup>-1</sup>.<sup>2</sup> The best-fit parameters (E mechanism) are  $E^0$  (Cc/Cc<sup>+</sup>)  $-0.8824$  V (vs. Ag/AgCl “leakless”, upper limit  $-0.8919$ , lower limit  $-0.8929$ , 95.4% confidence level), and  $k_{\text{et}} = 0.044$  cm s<sup>-1</sup> (upper limit 0.049, lower limit 0.039, 95.4% confidence level). The electrochemically-determined effective area of the platinum disk is 0.08 cm<sup>2</sup>.



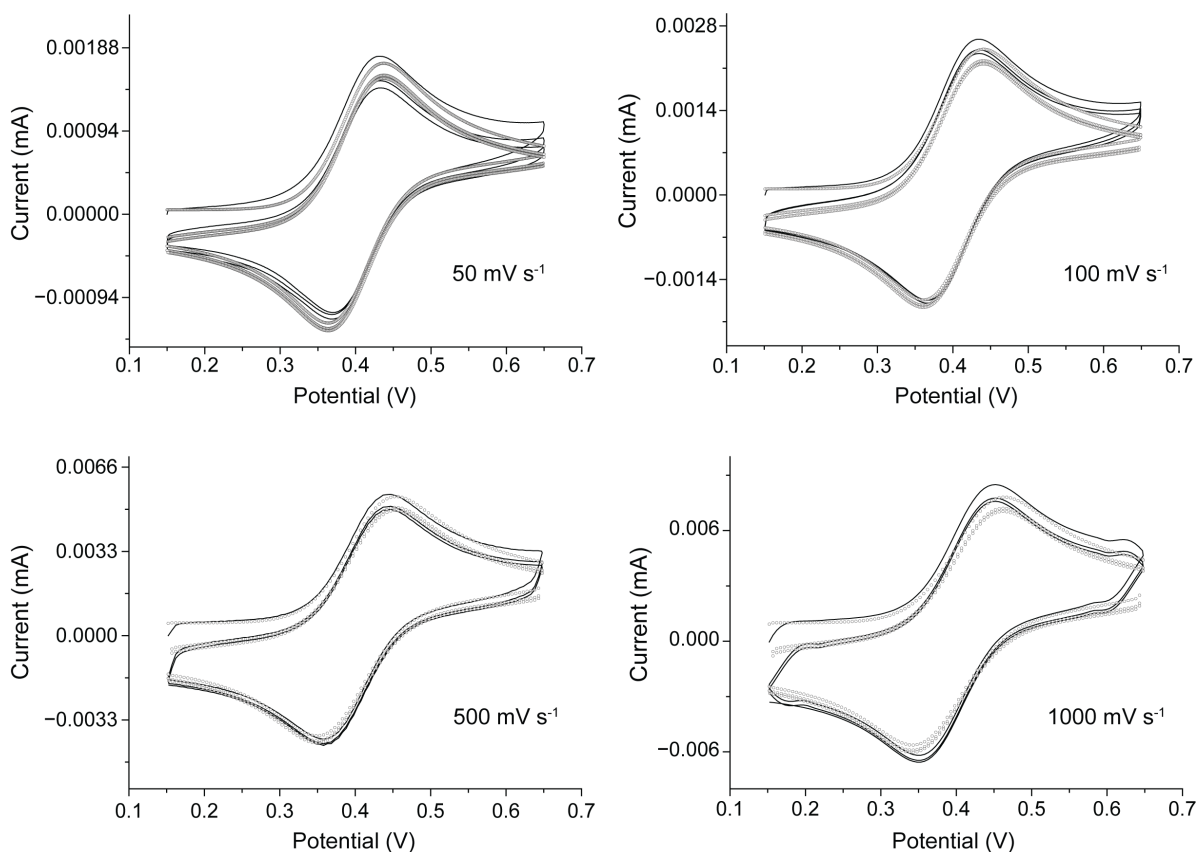


**Figure S16.** Representative experimental (solid line) and simulated (empty symbols) cyclic voltammograms at a platinum disk electrode in [EMIM][EtSO<sub>4</sub>] containing  $1.0 \times 10^{-3}$  M ferrocene. The voltage sweep rate is indicated by the labels to the figures. The best-fit parameters (E mechanism) are  $E^0$  (Fc/Fc<sup>+</sup>) = 0.4001 V (vs. Ag/AgCl “leakless”, upper limit 0.4000, lower limit 0.3998, 95.4% confidence level),  $k_{\text{et}} = 0.0011$  cm s<sup>-1</sup> (upper limit 0.0012, lower limit 0.0010, 95.4% confidence level), and  $D = 0.608 \times 10^{-7}$  cm<sup>2</sup> s<sup>-1</sup> (upper limit 0.611, lower limit 0.605, 95.4% confidence level). The electrochemically-determined effective area of the platinum disk is 0.08 cm<sup>2</sup>.

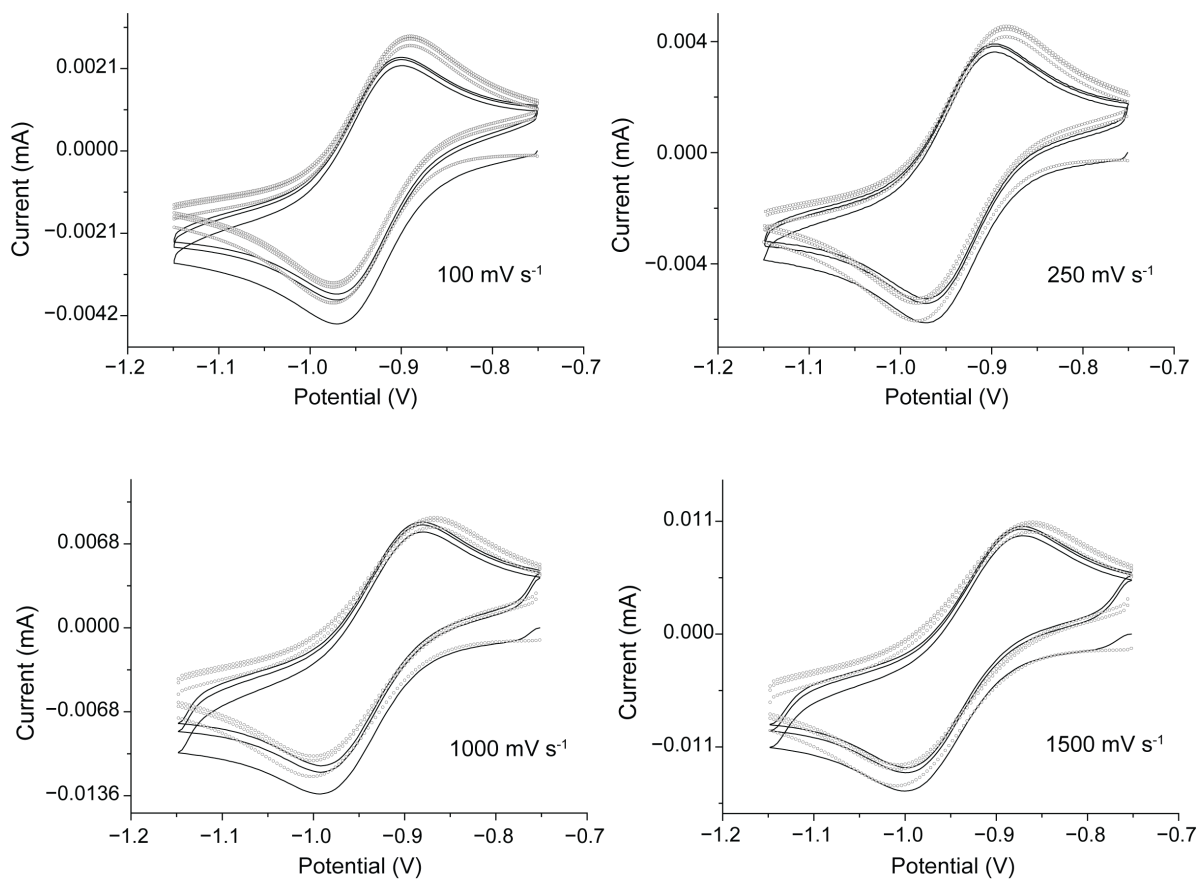


**Figure S17.** Representative experimental (solid line) and simulated (empty symbols) cyclic voltammograms at a platinum disk electrode in [EMIM][EtSO<sub>4</sub>] containing  $1.0 \times 10^{-3}$  M cobaltocenium hexafluorophosphate. The voltage sweep rate is indicated by the labels to the figures. The best-fit parameters (E mechanism) are  $E^0$  ( $Cc/Cc^+$ ) =  $-0.9317$  V (vs. Ag/AgCl “leakless”, upper limit  $-0.9307$ , lower limit  $-0.9327$ , 95.4% confidence level),  $k_{et} = 0.0019$  cm s<sup>-1</sup> (upper limit 0.0021, lower limit 0.0018, 95.4% confidence level), and  $D = 2.90 \times 10^{-7}$  cm<sup>2</sup> s (upper limit 2.93, lower limit 2.86, 95.4% confidence level). The electrochemically-determined effective area of the platinum disk is 0.08 cm<sup>2</sup>.

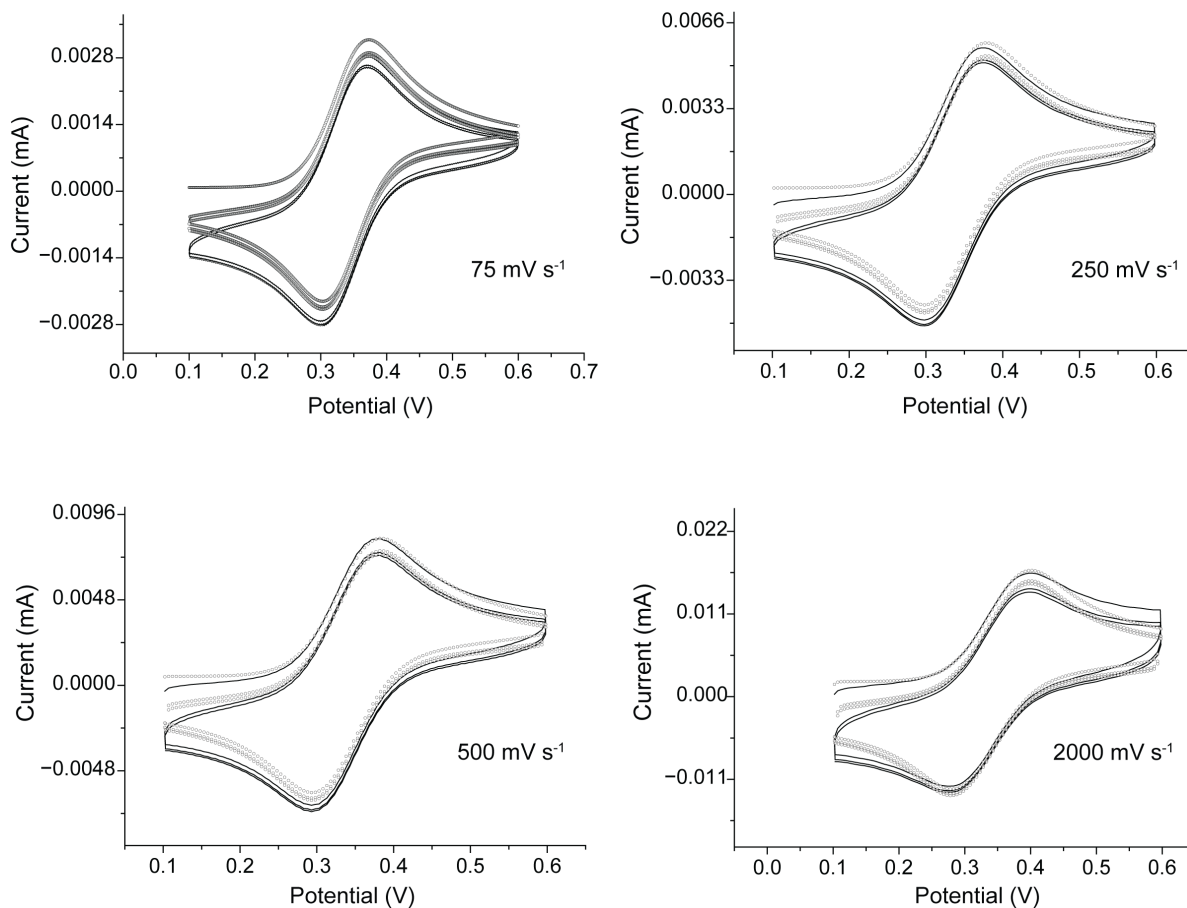


**Figure S18.** Representative experimental (solid line) and simulated (empty symbols) cyclic voltammograms at a platinum disk electrode in [BMPyrr][NTf<sub>2</sub>] containing  $1.0 \times 10^{-3}$  M ferrocene. The voltage sweep rate is indicated by labels to the figures. The best-fit parameters are (E mechanism)  $E^0$  (Fc/Fc<sup>+</sup>) was 0.3377 V (vs. Ag/AgCl “leakless”, upper limit 0.3382, lower limit 0.3373, 95.4% confidence level),  $k_{\text{et}} = 0.0046$  cm s<sup>-1</sup> (upper limit 0.0052, lower limit 0.0042, 95.4% confidence level), and  $D = 2.37 \times 10^{-7}$  cm<sup>2</sup> s<sup>-1</sup> (upper limit 2.41, lower limit 2.33, 95.4% confidence level). The electrochemically-determined effective area of the platinum disk is 0.08 cm<sup>2</sup>

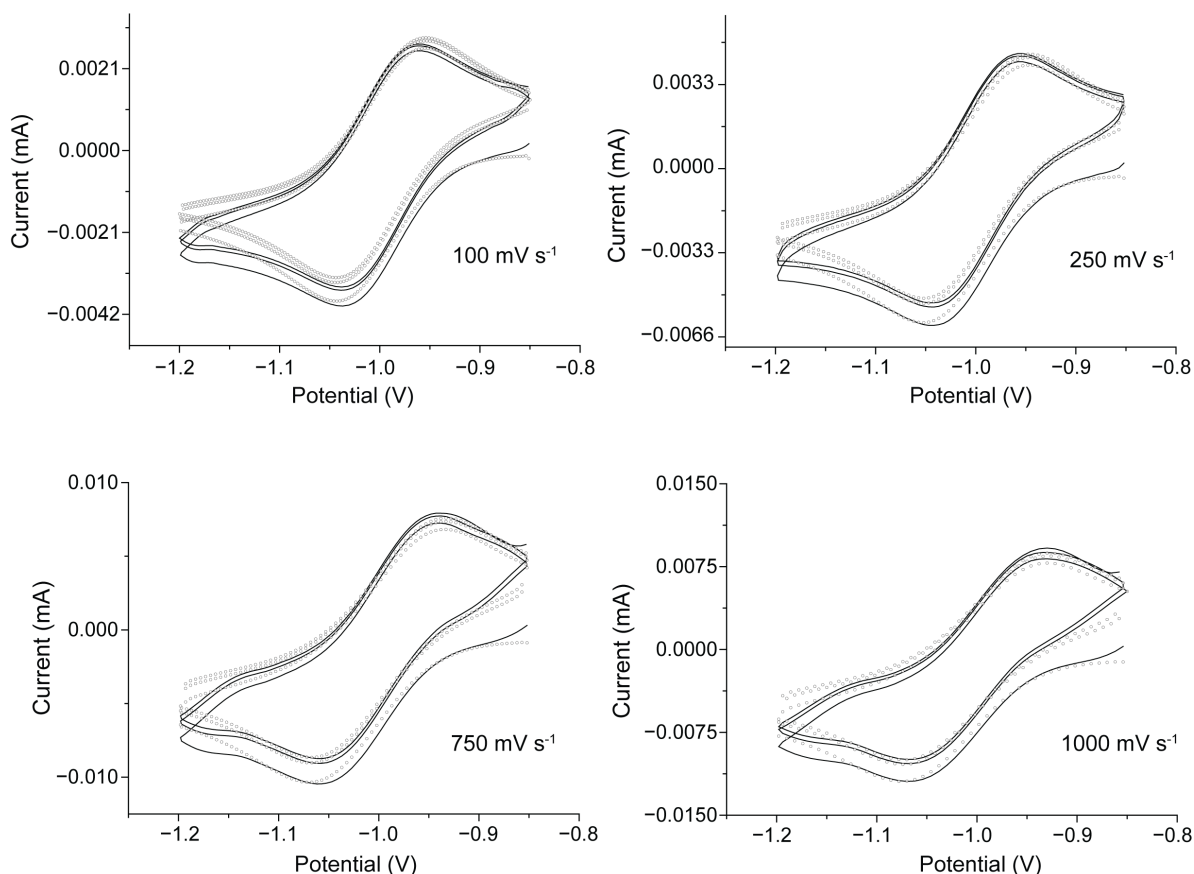


**Figure S19.** Representative experimental (solid line) and simulated (empty symbols) cyclic voltammograms at a platinum disk electrode in [BMPyr][NTf<sub>2</sub>] containing  $1.0 \times 10^{-3}$  M cobaltocenium hexafluorophosphate. The voltage sweep rate is indicated by labels to the figures. The best-fit parameters (E mechanism) are  $E^0$  (Cc/Cc<sup>+</sup>) =  $-0.9978$  V (vs. Ag/AgCl “leakless”, upper limit  $-0.9973$ , lower limit  $-0.9983$ , 95.4% confidence level),  $k_{\text{et}} = 0.0131$  cm s<sup>-1</sup> (upper limit 0.0136, lower limit 0.0126, 95.4% confidence level), and  $D = 1.92 \times 10^{-7}$  cm<sup>2</sup> s<sup>-1</sup> (upper limit 1.94, lower limit 1.90, 95.4% confidence level). The electrochemically-determined effective area of the platinum disk is 0.08 cm<sup>2</sup>.

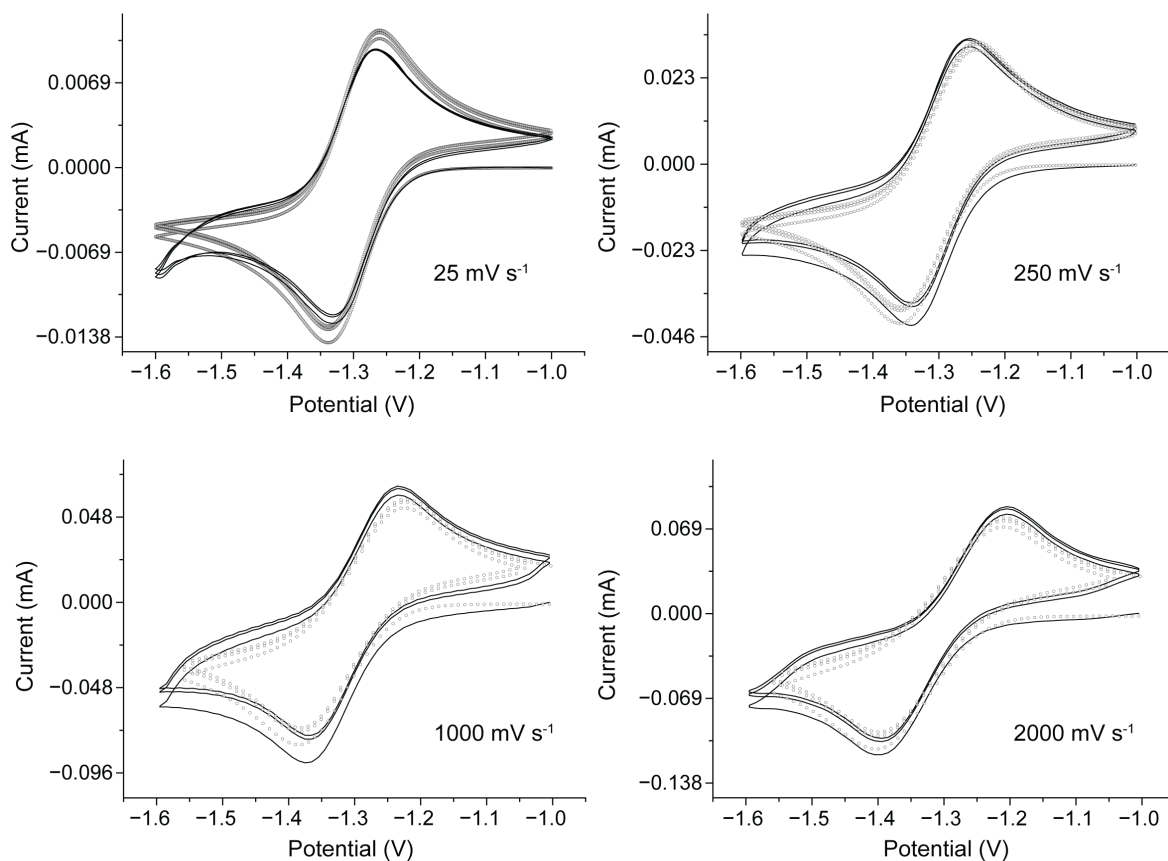


**Figure S20.** Representative experimental (solid line) and simulated (empty symbols) cyclic voltammograms at a platinum disk electrode in an acetonitrile solution containing  $1.0 \times 10^{-3}$  M decamethyl cobaltocenium hexafluorophosphate ( $\text{Me}_{10}(\text{Cc})^+$  hereafter) and  $1.0 \times 10^{-1}$   $\text{Bu}_4\text{NPF}_6$ . The voltage sweep rate is indicated by labels to the figures. The best-fit parameters (E mechanism) are  $E^0$  ( $\text{Me}_{10}(\text{Cc})/\text{Me}_{10}(\text{Cc})^+$ ) =  $-1.300$  V (vs.  $\text{Ag}/\text{AgCl}$  “leakless”, upper limit  $-1.299$ , lower limit  $-1.301$ , 95.4% confidence level),  $k_{\text{et}} = 0.016$   $\text{cm s}^{-1}$  (upper limit 0.017, lower limit 0.014, 95.4% confidence level), and  $D = 1.65 \times 10^{-5}$   $\text{cm}^2 \text{s}^{-1}$  (upper limit 1.67, lower limit 1.63, 95.4% confidence level). The electrochemically-determined effective area of the platinum disk is  $0.08$   $\text{cm}^2$ .

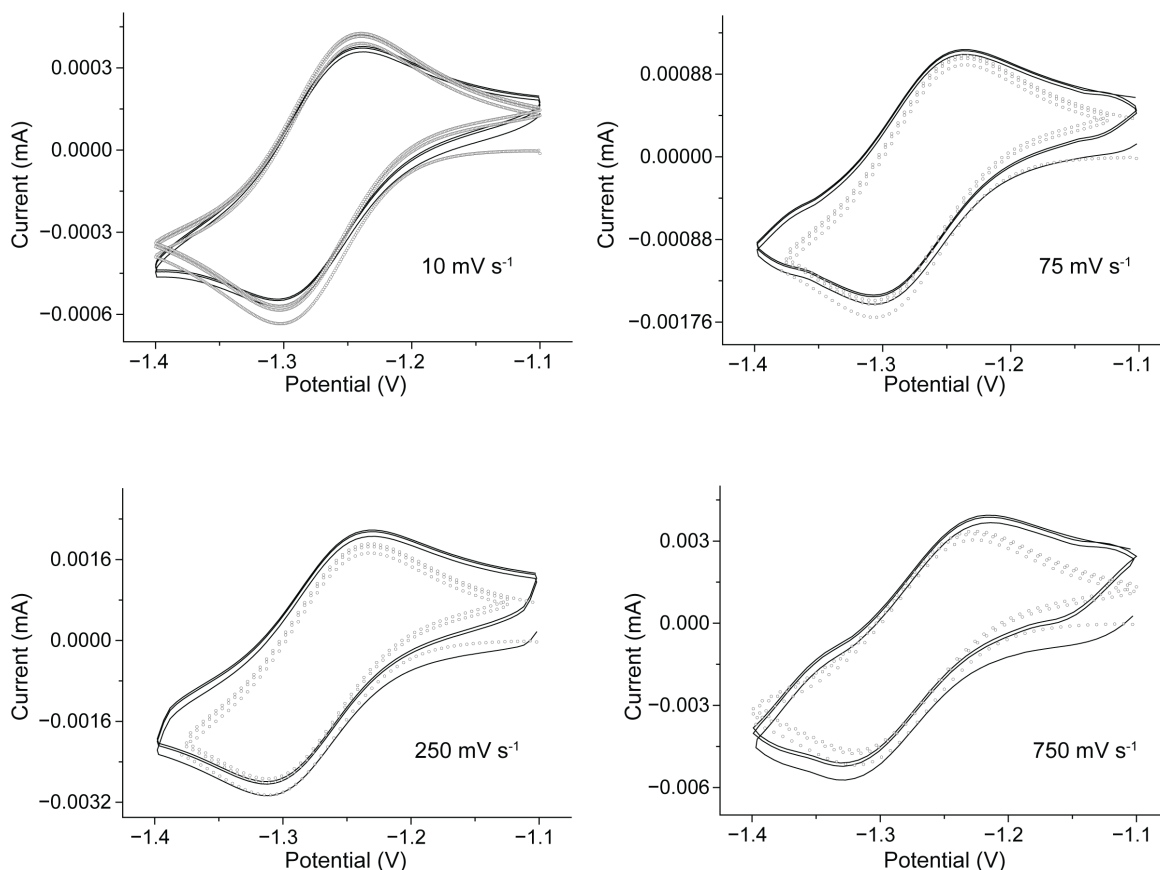


**Figure S21.** Representative experimental (solid line) and simulated (empty symbols) cyclic voltammograms at a platinum disk electrode in [EMIM][EtSO<sub>4</sub>] containing  $1.0 \times 10^{-3}$  M Me<sub>10</sub>(Cc)<sup>+</sup>. The voltage sweep rate is indicated by labels to the figures. The best-fit parameters (E mechanism) are  $E^0$  (Me<sub>10</sub>(Cc)/Me<sub>10</sub>(Cc)<sup>+</sup>) = -1.2729 V (vs. Ag/AgCl “leakless”, upper limit -1.214, lower limit -1.2724, 95.4% confidence level),  $k_{\text{et}} = 0.0023$  cm s<sup>-1</sup> (upper limit 0.0027, lower limit 0.0019, 95.4% confidence level), and  $D = 0.805 \times 10^{-7}$  cm<sup>2</sup> s<sup>-1</sup> (upper limit 0.816, lower limit 0.794, 95.4% confidence level). The electrochemically-determined effective area of the platinum disk is 0.08 cm<sup>2</sup>.

## Description of Supplementary Videos

### File name: Video S1

Time-stamped ECL emission recorded with a Nikon Eclipse Ti2-U inverted microscope fitted with a Plan Apo  $\lambda$  10 $\times$ /0.45 objective (part 88-379, Nikon, CFI Plan Fluor) and setting a 500 ms exposure time. A  $-2.0$  V bias was applied to the platinum mesh at the beginning of the video. The platinum mesh is immersed in an oxygen-saturated  $0.4 \times 10^{-3}$  M **AMP-luc** solution made in 0.2 M Bu<sub>4</sub>NClO<sub>4</sub>/DMSO. There was no emission filter. Selected video frames from this video are reproduced in Figure 1b of the main text.

### File name: Video S2

Time-stamped fluorescence recorded with a Nikon Eclipse Ti2-U inverted microscope fitted with a Plan Apo  $\lambda$  10 $\times$ /0.45 objective (part 88-379, Nikon, CFI Plan Fluor) and setting a 40 ms exposure time. A  $-2.0$  V bias was applied to the platinum mesh working electrode. The platinum mesh working electrode is immersed in an oxygen-saturated  $0.4 \times 10^{-3}$  M **AMP-luc** solution in [EMIM][EtSO<sub>4</sub>] (930 ppm). The microscope was fitted with a FITC filter/dichroic mirror cube (461.0–487.5 nm excitation filter, 502.5–547.5 nm emission filter) was used. Selected video frames from this video are reproduced in Figure 2a–c of the main text.

### File name: Video S3

Time-stamped fluorescence recorded with a Nikon Eclipse Ti2-U inverted microscope fitted with a Plan Apo  $\lambda$  10 $\times$ /0.45 objective (part 88-379, Nikon, CFI Plan Fluor) and setting a 40 ms exposure time. A  $-2.0$  V bias was applied to the platinum mesh. The platinum mesh working electrode is immersed in an oxygen-saturated  $0.4 \times 10^{-3}$  M **AMP-luc** solution in [EMIM][BF<sub>4</sub>] (2400 ppm). The microscope was fitted with a FITC filter/dichroic mirror cube (461.0–487.5 nm excitation filter, 502.5–547.5 nm emission filter). Selected video frames from this video are reproduced in Figure 3a–b of the main text.

### File name: Video S4

Time-stamped ECL emission recorded with a Nikon Eclipse Ti2-U inverted microscope fitted with a Plan Apo  $\lambda$  10 $\times$ /0.45 objective (part 88-379, Nikon, CFI Plan Fluor) and setting a 1 s exposure time. A  $-2.0$  V bias was applied to the platinum mesh. The platinum mesh working electrode is immersed in an oxygen-saturated  $0.4 \times 10^{-3}$  M **AMP-luc** solution in 0.2 M Bu<sub>4</sub>NClO<sub>4</sub>/DMSO. No emission filter was used. Selected video frames from this video are reproduced in Figure S4a–c, Supporting Information.

### File name: Video S5

Time-stamped fluorescence recorded with a Nikon Eclipse Ti2-U inverted microscope fitted with a Plan Apo  $\lambda$  10 $\times$ /0.45 objective (part 88-379, Nikon, CFI Plan Fluor) and setting a 40 ms

exposure time. A  $-2.0$  V bias was applied to the platinum mesh at the beginning of the video. The platinum mesh working electrode is immersed in a  $0.4 \times 10^{-3}$  M **AMP-luc** solution in [BMPyrr][NTf<sub>2</sub>] (125 ppm). A FITC filter/dichroic mirror cube (461.0–487.5 nm excitation filter, 502.5–547.5 nm emission filter) was used. Selected video frames from this video are reproduced in Figure S5a–c, Supporting Information.

**File name: Video S6**

Time-stamped fluorescence recorded with a Nikon Eclipse Ti2-U inverted microscope fitted with a Plan Apo  $\lambda$  10 $\times$ /0.45 objective (part 88-379, Nikon, CFI Plan Fluor) and setting a 40 ms exposure time. A  $-2.0$  V bias was applied to the platinum mesh. The platinum mesh working electrode is immersed in an oxygen-saturated  $0.4 \times 10^{-3}$  M **AMP-luc** solution in [EMIM][EtSO<sub>4</sub>] spiked with 2% of water. The microscope was fitted with a FITC filter/dichroic mirror cube (461.0–487.5 nm excitation filter, 502.5–547.5 nm emission filter). Selected video frames from this video are reproduced in Figure S7a, Supporting Information.

**File name: Video S7**

Time-stamped fluorescence recorded with a Nikon Eclipse Ti2-U inverted microscope fitted with a Plan Apo  $\lambda$  10 $\times$ /0.45 objective (part 88-379, Nikon, CFI Plan Fluor) and setting a 40 ms exposure time. A  $-2.0$  V bias was applied to the platinum mesh. The platinum mesh working electrode is immersed in an oxygen-saturated  $0.4 \times 10^{-3}$  M **AMP-luc** solution in [EMIM][EtSO<sub>4</sub>] spiked with 5% of water. A FITC filter/dichroic mirror cube (461.0–487.5 nm excitation filter, 502.5–547.5 nm emission filter) was used. Selected video frames from this video are reproduced in Figure S7c, Supporting Information.

**File name: Video S8**

Time-stamped fluorescence recorded with a Nikon Eclipse Ti2-U inverted microscope fitted with a Plan Apo  $\lambda$  10 $\times$ /0.45 objective (part 88-379, Nikon, CFI Plan Fluor) and setting a 40 ms exposure time. A  $-2.0$  V bias was applied to the platinum mesh. The platinum mesh working electrode is immersed in a  $0.4 \times 10^{-3}$  M **AMP-luc** solution in [BMPyrr][NTf<sub>2</sub>] spiked with 2% of water. The microscope was fitted with a FITC filter/dichroic mirror cube (461.0–487.5 nm excitation filter, 502.5–547.5 nm emission filter) was used. Selected video frames from this video are reproduced in Figure S7e, Supporting Information.



## References

1. Bond, A. M.; Oldham, K. B.; Snook, G. A., Use of the Ferrocene Oxidation Process To Provide Both Reference Electrode Potential Calibration and a Simple Measurement (via Semiintegration) of the Uncompensated Resistance in Cyclic Voltammetric Studies in High-Resistance Organic Solvents. *Anal. Chem.* **2000**, *72*, 3492–3496.
2. Tsierkezos, N. G., Electron transfer kinetics for the cobaltocene (+1/0) couple at platinum disk electrode in acetonitrile/dichloromethane binary solvent system. *J. Mol. Liq.* **2008**, *138*, 1–8.